Published in final edited form as:
Atherosclerosis. 2010 December ; 213(2): 449–457. doi:10.1016/j.atherosclerosis.2010.09.030.

Two adjacent domains (141-150 and 151-160) of apoE covalently linked to a class A amphipathic helical peptide exhibit opposite atherogenic effects

Gaurav Nayyar, **Shaila P. Handattu**, **Candyce E. Monroe**, **Manjula Chaddha**, **Geeta Datta**, **Vinod K. Mishra**, **Tamara D. Keenum**, **Mayakonda N. Palgunachari**, **David W. Garber**, and **G.M. Anantharamaiah**
Atherosclerosis Research Unit and the Department of Medicine, Biochemistry and Molecular Genetics, University of Alabama at Birmingham, Birmingham, AL35294

Abstract

Objective—We recently described anti-atherogenic properties of the dual domain peptide Ac-hE18A-NH_2 derived by covalently linking the heparin binding domain 141-150 of apoE to 18A, a class A amphipathic helical peptide. In this paper we have compared the properties of Ac-hE18A-NH_2 with the non-heparin binding 151-160 region of apoE linked to 18A (Ac-nhE18A-NH_2).

Methods and Results—Both peptides were highly helical in solution and in association with lipids. Ac-hE18A-NH_2 and not Ac-nhE18A-NH_2 enhanced uptake of low density lipoprotein (LDL) in HepG2 cells. While Ac-hE18A-NH_2 retarded the electrophoretic mobility of LDL, Ac-nhE18A-NH_2 slightly enhanced mobility. Ac-hE18A-NH_2 reduced monocyte association with endothelial cells, while Ac-nhE18A-NH_2 increased it. Ac-hE18A-NH_2 also reduced lipid hydroperoxide content of LDL while Ac-nhE18A-NH_2 increased it. A single administration of Ac-hE18A-NH_2 (100 μg/mouse) into apoE null mice dramatically reduced cholesterol (from 600 mg/dL to 180 mg/dL at five min. and to 60 mg/dL at five h) while Ac-nhE18A-NH_2 had no effect. Administration (100μg/mouse/day, three days a week) into apoE null mice for six weeks showed Ac-hE18A-NH_2 group having a moderate aortic sinus lesion reduction compared with the control group (−15.1%), while the Ac-nhE18A-NH_2 administered group had increased lesion area (+33.0% vs controls and 36.1% vs Ac-hE18A-NH_2). Plasma from mice administered Ac-hE18A-NH_2 for six weeks showed a significant reduction in plasma cholesterol and triglyceride levels and increase in paraoxonase-1 (PON-1) activity compared to controls, while Ac-nhE18A-NH_2 caused no change in plasma cholesterol and decreased PON-1 activity.

Conclusion—It is proposed that Ac-hE18A-NH_2 reduced lesion progression in apoE null mice due to its anti-inflammatory and lipoprotein clearing properties, while Ac-nhE18A-NH_2 exhibited pro-atherogenic effects.

Keywords

Atherosclerosis; Lipid oxidation; Apolipoproteins; Cholesterol; Peptides

Address for Correspondence: David W. Garber, Ph.D. University of Alabama at Birmingham, 1808 7th Ave. S. BDB Room D-654, Birmingham, AL-35294, Dgarber@uab.edu, 205-934-1218.
Gaurav Nayyar and Shaila P. Handattu contributed equally to this work.

1. Introduction

The importance of apolipoprotein E (apoE) for clearing plasma cholesterol and inhibiting atherosclerosis has been demonstrated in an animal model by removal of the apoE gene in mice, which produces atherosclerosis spontaneously with plasma containing high levels of very low density lipoprotein- (VLDL) like cholesterol rich particles (1,2) Over-expression of apoE in animals decreases circulating cholesterol levels (3). Addition of apoE to VLDL enhances uptake and degradation of VLDL (4), which is known to carry more cholesterol per particle than LDL; both of these apoB-containing lipoproteins are atherogenic (5). ApoE acts as a ligand for several receptors, including the LDL-receptor (LDLR) and the LDL receptor-related protein (LRP). Binding of apoE-containing lipoproteins to heparan sulfate proteoglycans (HSPG), and lipoprotein lipase mediates binding of apoE-containing lipoproteins, acting to clear LDL and VLDL in the space of Disse (6). The region 141-160 of human apoE possesses a cationic putative receptor binding domain with the residue Cys at 158 of apoE2 replaced by Arg in isoform E3, the major allelic form that is present in normolipidemic individuals (7). While the region 141-150 (LRKLRKRLLR) is highly cationic with six out of ten residues consisting of positively charged residues and the other residues being hydrophobic Leu, region 151-160 (DADDLQKRLA) is also rich in charged residues (5 out of 10) but possesses a 3:2 negative to positive charge ratio.

Our earlier studies to design an apoE mimetic peptide considered the dual domain structural pattern present in apoE in which the N-terminal 4-helix bundle region is connected to a long class A amphipathic helix (8). The classic work of Bradley and Gianturco showed that in the absence of the lipid associating domain, the putative receptor binding domain at the N-terminal region does not associate with lipoprotein surfaces to enhance the clearance of atherogenic lipoproteins (8). Based on this idea, we designed the dual domain peptide in which the putative receptor binding region of 141-150 of apoE (LRKLRKRLLR, abbreviated as hE) is covalently linked to the model class A amphipathic helical peptide 18A (with the sequence DWLKAFYDKVAEKLKEAF; 9, 10) to obtain Ac-hE18A-NH_2. This peptide is able to associate with apoB-containing atherogenic lipoproteins and enhance their hepatic uptake and degradation *via* HSPG on the surface of hepatocytes. This results in a dramatic reduction of plasma lipoproteins in dyslipidemic animal models (11,12,13). Additionally, similar to apoE, peptide Ac-hE18A-NH_2 was shown to recycle, form preβ HDL-like particles, enhance paraoxonase-1 (PON-1) activity, and improve endothelial function (13,14). In this paper we have examined the effect of this peptide on atherosclerotic plaque formation in apoE null mice.

A second peptide was synthesized by covalently attaching the 151-160 region of apoE to 18A to obtain Ac-nhE18A-NH_2 in which nhE represents the non-heparin binding domain DADDLQKRLA (15). In this paper we have compared the physical/chemical and atheroprotective potential of these two peptides *in vitro* and *in vivo* using the apoE null mouse model. The results show that while the peptide Ac-hE18A-NH_2 is able to decrease plasma cholesterol levels, increase PON-1 activity, and reduce lesion formation, the peptide Ac-nhE18A-NH_2 did not decrease plasma cholesterol levels, decreased PON-1 activity and increased atherosclerosis.

2. Materials and Methods

2.1. Synthesis of peptides

Peptides were synthesized as described previously (16) using solid phase peptide synthesis method. Purity of the peptides was assessed by analytical HPLC and mass spectral analysis. Peptide Ac-hE18A-NH_2 had the amino acid sequence LRKLRKRLLR-DWLKAFYDKVAEKLKEAF, while Ac-nhE18A-NH_2 had the sequence DADDLQKRLA-

DWLKAFYDKVAEKLKEAF, with the hyphens designating the delineation between the apoE sequences and the sequence from peptide 18A. The amino and carboxy terminus of each peptide was protected by acetyl and amide groups, respectively.

2.2. Phospholipid turbidity clarification measurements

Association of these peptides with palmitoyloleoyl phosphatidylcholine (POPC) was determined by following the dissolution of POPC multilamellar vesicles (MLV) by reduction in turbidity using a plate reader (Bio-Tek Synergy HT). POPC MLVs were prepared by evaporating a chloroform/methanol (2/1) solution of POPC (Avanti Polar Lipids) under nitrogen and hydrating the lipid film with phosphate buffered saline (pH 7.4). The sample containing 100 μM of POPC and an equimolar amount of peptide was maintained at room temperature and continuously agitated. Turbidity clarification was monitored at 400 nm for 50 min. As a positive control, the ability of Triton X-100 (1%) to clarify POPC was measured.

2.3. Circular Dichroism (CD) studies

CD spectra were recorded on a signal-averaging AVIV 62DS spectropolarimeter as described previously (9). Briefly, CD spectra were obtained at 25°C by signal averaging of four scans recorded every nanometer from 260 nm to 190 nm using a cell with a 0.01cm path length. Peptide concentrations were 10 to 100 μM in PBS (pH 7.4). Peptide:DMPC complexes (1:20 mol:mol) were prepared as described previously (9) and the change in peptide helicity upon lipid association was measured. The helical content of the peptides was estimated from the mean residue ellipticity $[Ø]_{MRE}$ (deg. cm^2dmol^{-1}) at θ_{222} using the equation described in detail by Morrisett et al (17).

2.4. Monocyte Adhesion Assay

Peptides (50μg/ml) or vehicle were mixed with 1 ml of human blood for 30 min at 37° and cells were removed by centrifugation. HDL was separated by sequential density ultracentrifugation as described previously (18). This HDL fraction was then used to analyze anti-inflammatory properties of the peptide using the BAEC (bovine aortic endothelial cells) assay (14,19). BAECs were grown to 80% confluence in 24 well plates. They were treated with medium alone, lipopolysaccharide (LPS; 1 μg/ml, as a positive control) or 200 μl of human HDL or HDL isolated from blood that was treated with either vehicle or peptide (Ac-hE18A-NH_2 or Ac-nhE18A-NH_2) and incubated for 6h. Concurrently THP-1 monocytes were labeled with calcein as per the manufacturer's instructions (Molecular Probes). After 6h, the BAECs were washed with PBS and incubated with labeled monocytes for 1h at 37°C. The cells were washed and fluorescence was measured using an excitation wavelength of 495 nm and an emission at 517 nm.

2.5. Internalization of LDL by HepG2 cells

LDL was isolated from human plasma by sequential density ultracentrifugation (18). The uptake of [^{125}I]LDL in the presence of peptides to HepG2 cells was done using the method of Goldstein et al (20). LDL was labeled with ^{125}I using the Iodogen method (Thermo Fisher Inc., Rockford IL). Cells were grown in 10% fetal bovine serum (FBS) and penicillin-streptomycin-amphoterecin in 6 well plates and used after reaching 75 to 90% confluence (2 to 3 days). The seeding density of cells used was 1.5×10^5 cells/ml medium. Cells were incubated with medium containing lipoprotein deficient serum for 24h prior to use. Uptake (or internalization) was measured in cells incubated at 37°C for 2h. After washing four times with ice cold PBS containing 2mg/ml BSA to remove nonspecifically bound lipoprotein, the cells were incubated with dextran sulfate (4 mg/ml, Pharmacia Mr wt 500,000) for 1h to release specifically bound [^{125}I]LDL. The counts in the dextran sulfate wash reflected the

amount of LDL bound to cells. The cells were washed with cold PBS, dissolved in 1 ml 0.1N NaOH and 0.5 ml aliquot was counted. The counts reflect the amount of LDL internalized. Protein was measured by the method of Lowry et al (21). In all the cell experiments, mean values from replicate measurements of three independent experiments were used.

2.6. Measurement of lipid hydroperoxides

Human LDL was mixed with peptides at a 1:1 ratio and incubated at 37°C overnight. Lipid hydroperoxide levels were measured using the CHOD-iodide method (22); spectrophotometric measurements were made at a wavelength of 365 nm.

2.7. Effect of intravenous administration of peptides on plasma cholesterol in apoE null mice

Female apoE null mice were purchased from Jackson Laboratories (Bar Harbor MI) at 14 weeks of age. After acclimatization for two weeks they were randomized into three groups. Peptides Ac-hE18A-NH_2 and Ac-nhE18A-NH_2 (100μg/100 μl in saline/mouse) were administered retro-orbitally three times a week for six weeks. The control group received 100 μl of saline. Blood was collected from retro-orbital sinus under anesthesia at time points mentioned in the figures and cholesterol measured manually using commercially available kits (Infinity Cholesterol Reagent, Thermo Scientific). All animal studies were performed using the protocols approved by the Institutional Animal Care and Use Committee of The University of Alabama at Birmingham.

2.8. The role of HSPG in peptide Ac-hE18A-NH_2-mediated clearance of apoB-containing lipoproteins

Peptide Ac-hE18A-NH_2 associates with apoB-containing lipoproteins (11,12). To determine if this peptide associates with hepatic HSPG and targeting them to the liver for clearance, we followed the procedure of Mahley et al (23). In brief, HSPG was blocked by administering heparinase either before or after administering Ac-hE18A-NH_2. In pre-treatment of heparinase, female apoE null mice were administered with either saline or heparinase (50 U/mouse). 5 min. later, all the animals received Ac-hE18A-NH_2 (100 μg/mouse, i.v). Blood was drawn at various time points for plasma cholesterol analysis. In heparinase post-treatment experiment, ^{125}I-labeled Ac-hE18A-NH_2 (100 μg/mouse, i.v) was administered to female apo E null mice. 15 min. later half the animals received saline and the other half received heparinase (50 U/mouse). Blood was drawn at various time points to monitor plasma cholesterol levels and disappearance of radioactivity from plasma. Similar experiments were not done with Ac-nhE18A-NH_2 as it had no effect on LDL uptake by hepatocytes (Fig. 2a) or reduction of plasma cholesterol (Fig. 3b).

2.9. Lesion Quantification

At the end of six weeks blood samples were taken under anesthesia by cardiac puncture, and hearts were excised and subjected to histological examination and quantification of lesion area as described earlier (24). In brief, hearts were fixed for at least 1 week in the phosphate-buffered formaldehyde solution. After the lower two-thirds of the hearts were removed, the remaining tissue was frozen in freezing medium (OCT Tissue-Tek; Miles Laboratories Ltd, Elkhart, IN) and sectioned in a cryostat at −20°C. Alternate 10-μm sections were saved on slides and observed for the beginning of the aortic root. Sections were then collected for an additional 600 μm, or until the aortic cross section was rounded and the valve cusps were no longer evident. Slides were stained with Oil Red O, and counterstained with hematoxylin. Stained lesion cross-sectional areas were measured in consecutive slides 80 μm apart by image analysis (SigmaScan Pro; SPSS Science, Chicago, IL), and the average lesion area

was determined for each aortic sinus over the 400-μm length (five slides) providing the greatest mean lesion area. *En face* preparations of the entire aorta from the aortic arch to the iliac bifurcation (25) were done in mice treated with Ac-hE18A-NH_2. The aorta was excised, cleaned, and opened longitudinally with extremely fine Vannas scissors, then pinned flat on a black wax surface. The aorta was then stained Oil Red O and lesions were quantified by video capture under a stereo dissecting microscope. Lesion and total areas were determined using SigmaScan (Systat) and lesion area was expressed as a percentage of total area.

2.10. PON-1 activity

PON-1 activity in plasma was measured as described earlier (13). In brief, 2 μl of plasma was added to 200 μl of buffer (100mmol/L Tris containing 2 mmol/L $CaCl_2$, pH 8.0) containing paraoxon (1 mmol/L *O*,*O*-diethyl-*O*-*p*-nitrophenylphosphate), and the rate of release of 4-nitrophenol was determined spectrophotometrically. The assay was performed in a 96-well plate, and readings were taken every 2 minutes at 405 nm. The quantity of 4-nitrophenol formed was calculated using the molar extinction coefficient of 17100 mol/$L^{-1}cm^{-1}$and PON-1 activity was expressed as nmoles of 4-nitrophenol formed per minute.

2.11. Statistics

Groups were compared by one-way analysis of variance (ANOVA) when the data were normally distributed or one-way ANOVA on ranks when normality failed. Post-hoc analyses were by two-tailed Student's t-test. Where two groups were tested, analysis was done using two-tailed Student's t-test. Groups were considered significantly different when $p<0.05$.

3. Results

3.1. Secondary structures and association of peptides with lipoproteins

In Ac-hE18A-NH_2, due to the presence of additional Leu residues in LRKLRKRLLR, the hydrophobic face is extended by two more residues but the helical net representation of Ac-hE18A-NH_2 shows that the hydrophobic face is twisted by 180°. In the helical wheel representation, despite the presence of the class A amphipathic helical peptide 18A, addition of 141-150, did not show the amphipathic helical nature of the peptide (Fig. 1). Despite this, the peptide Ac-hE18A-NH_2 associates strongly with phospholipids and atherogenic lipoproteins (9,12). On the other hand, addition of residues 151-160 from the apoE putative receptor binding domain to 18A extended and maintained the class A amphipathic helical nature of Ac-nhE18A-NH_2 with a wide nonpolar face rich in Leu residues (Fig. 1). CD studies indicated that the peptides have similar helical content both in solution and when associated with lipid. Based on mean residue ellipticity at 222 nm, Ac-nhE18A-NH_2 is 78% helical in solution and 80% helical when associated with lipid; Ac-hE18A-NH_2 is 69% helical in solution and 74% helical when associated with lipid.

Physical properties of the peptides are shown in Table 1. These demonstrate that, compared to Ac-hE18A-NH_2, Ac-nhE18A-NH_2 is more amphipathic (higher hydrophobic moment/residue) and more hydrophobic (overall hydrophobicity/residue). However, hydrophobicity of the nonpolar face is higher for Ac-hE18A-NH_2 than Ac-nhE18A-NH_2. The predicted lipid affinity (λ4) of Ac-nhE18A-NH_2 is higher than Ac-hE18A-NH_2. It is important to note that while Ac-hE18A-NH_2 is overall positively charged (net charge +6), Ac-nhE18A-NH is overall negatively charged (−1).

Association of peptides with multilamellar POPC vesicles converts turbid suspensions into clear solutions due to peptide:lipid complex formation (10,26). As shown in Fig, 2a, addition of either peptide to MLVs of POPC clarifies these vesicles to form peptide:lipid complexes.

These results indicate that the peptides are capable of associating with lipoproteins. Incubation of human LDL with both peptides altered agarose electrophoretic mobility indicating both the peptides interacted with LDL. While Ac-hE18A-NH_2 reduced the electrophoretic mobility of LDL due to increased positive charges associating with the LDL surface, Ac-nhE18A-NH_2 slightly enhanced electrophoretic mobility (Fig. 2b). At the higher LDL:Ac-hE18A-NH_2 ratio the effect on LDL mobility was greater, but the effect of Ac-nhE18A-NH_2 was similar at both ratios

3.2. Effects of peptides on LDL uptake by cultured hepatocytes

To determine the effects of these two peptides on uptake of LDL to HepG2 cells, human LDL was incubated with peptides (at 1:1 w:w ratio) and re-isolated by sequential density centrifugation as described previously (9). As shown in Fig. 3a, peptide Ac-hE18A-NH_2 enhanced LDL uptake by HepG2 cells by four times compared with controls while the peptide Ac-nhE18A-NH_2 did not enhance LDL uptake by HepG2 cells.

3.3. Effects of peptides on HDL anti-inflammatory properties

Effects of peptides on HDL anti-inflammatory properties were determined by analyzing the effect of peptide-treated HDL on binding of monocytes to BAEC. This assay was developed in our laboratory (14,19). LPS was used as a positive control as LPS is known to increase adhesion of monocytes to endothelial cells as shown in Fig. 3b. HDL isolated from blood incubated with peptide Ac-hE18A-NH_2 inhibited binding of monocytes to BAECs compared with HDL alone (Ac-hE18A-NH_2, 2729±141; HDL, 4473±118 units; $p<0.002$), whereas Ac-nhE18A-NH_2 did not exhibit this effect (4861±118 units; $p<0.001$ vs Ac-hE18A-NH_2).

3.4. Effect of peptides on LDL lipid hydroperoxides

After incubation of human LDL with peptides or vehicle overnight at 37°C, lipid hydroperoxide levels were markedly and significantly increased in LDL incubated with Ac-nhE18A-NH_2 (LDL, 0.057±0.001; Ac-nhE18A-NH_2, 0.127±0.000 absorbance units; $p<0.001$), while they were significantly decreased in LDL incubated with Ac-hE18A-NH_2 (0.029±0.006; $p<0.001$ vs LDL; Fig. 3c).

3.5. Acute effect of peptides on plasma cholesterol levels and involvement of heparan sulfate proteoglycans

To determine the effect of peptides Ac-nhE18A-NH_2 and Ac-hE18A-NH_2 on plasma cholesterol levels, the peptides (100μg/mouse) were administered intravenously to female apo E null mice. Blood was drawn before administration, 5 min and 5 hrs post-administration for plasma cholesterol analysis. As shown in Fig. 4a, mice administered with Ac-hE18A-NH_2 showed a dramatic decrease in plasma cholesterol levels at both the 5 min and 5 hr time points, unlike mice administered with either saline or Ac-nhE18A-NH_2 which had similar changes in plasma cholesterol levels. Thus, peptide Ac-nhE18A-NH_2 which does not possess the cholesterol lowering capacity of Ac-hE18A-NH_2 was used as a negative control for further experiments.

Next, we analyzed whether, analogous to apoE, HSPG is involved in Ac-hE18A-NH_2-mediated lipoprotein clearance from plasma. We administered heparinase (which removes HSPG from cell surfaces) either before or after injecting peptide Ac-hE18A-NH_2 to apo E null mice. Fig. 4b shows that pre-treatment of heparinase followed five minutes later by injection of Ac-hE18A-NH_2 abolishes the cholesterol lowering ability of the peptide compared to mice pre-treated with saline. These results were apparently not due to peptide inhibition of heparinase activity (Supplemental Fig. 1). Thus, Ac-hE18A-NH_2-mediated lipoprotein clearance is mainly through HSPG. Next, we analyzed if post treatment of

heparinase would release the peptide or lipoproteins bound to HSPG. We injected [^{125}I]Ac-hE18A-NH_2 (100μg/mouse, i.v.) to female apoE null mice. 15 min. later, half the animals received saline and the other half received heparinase (50 U/mouse). Plasma cholesterol and radioactivity was followed at various time points. As shown in Fig. 4c, plasma cholesterol levels decreased similarly in both groups and disappearance of the peptide from plasma was also similar. The majority of the radioactivity was found in the liver (saline controls: 60.13±5.37% and peptide-injected: 59.87±4.19% of injected radioactivity in liver. N=5 in each group.). Radioactivity in the aorta was not distinguishable from background. Similar results were obtained when heparinase was injected 5 minutes after peptide (data not shown). This suggests that association of Ac-hE18A-NH_2-mediated apoB-containing lipoproteins is rapid and not readily reversible.

3.6. Effect of chronic administration of peptides on plasma cholesterol and triglyceride levels and paraoxonase-1 (PON-1) activity

Peptide solutions were prepared in sterile saline and were injected into apoE null mice 3 times a week for 6 weeks. Both the peptides were administered retro-orbitally at the dose of 100 μg three times per week. Blood was drawn before the initiation of the treatment regimen and at the end of experiment. Final plasma samples were taken 24 hours after the last peptide administration. Plasma was analyzed for cholesterol and triglyceride levels and PON-1 activity. As shown in Fig. 5a, plasma cholesterol levels of Ac-nhE18A-NH_2 treated mice did not change significantly from that of the control group after 6 weeks of administration, whereas Ac-hE18A-NH_2 treated mice had significantly lower plasma cholesterol levels compared to both control and Ac-nhE18A-NH_2 treated mice. The reduction in plasma cholesterol was largely in the VLDL region, while the HDL region had a slight but significant increase in the Ac-hE18A-NH_2 group compared with the other groups (Supplemental Fig. 2). Plasma triglyceride levels were also reduced in the Ac-hE18A-NH_2 treated mice compared with either the control or Ac-nhE18A-NH_2 groups (Fig. 5b). Next we analyzed the plasma samples (after treatment) for PON-1 activity. As shown in Fig 5c, mice treated with Ac-hE18A-NH_2 showed a significant increase in PON-1 activity compared to both the groups, whereas treatment with Ac-nhE18A-NH_2 resulted in decreased paraoxonase activity, thus indicating that this peptide could be pro-inflammatory.

3.7. Effects of Ac-hE18A-NH_2 and Ac-nhE18A-NH_2 on atherosclerotic lesions

After 6 weeks of peptide administration aortic root sections were analyzed for atherosclerotic lesions using Oil Red O staining. Fig 6a shows mean lesion areas in the three groups. Compared to the Ac-nhE18A-NH_2 group, Ac-hE18A-NH_2 administration resulted in significant inhibition of atherosclerotic lesion formation. However, Ac-nhE18A-NH_2 treated mice showed significantly increased plaque formation compared to the control group. Thus, while Ac-hE18A-NH_2 had a trend towards decreased lesion area compared with controls (−15.1%), and significantly less lesion area compared with peptide Ac-nhE18A-NH_2 (−36.1%; $p<0.0.001$), the latter peptide was pro-atherogenic compared with controls (+33.0%; $p<0.001$).

The lesion reduction in the group treated with Ac-hE18A-NH_2 did not reach significance compared with controls, perhaps due to the large lesion area in the aortic sinus in all groups. In a separate experiment intended to confirm the atheroprotective properties of this peptide, 22 week old female apoE null mice were injected with either saline (n=11) or Ac-hE18A-NH_2 (n=12; 100μg/mouse, 3 times a week) for 4 weeks by retro-orbital administration. After 4 weeks, the animals were anaesthetized, perfused with saline, and the aorta was harvested from the aortic arch to iliac bifurcation. The aorta was cut open, pinned onto a black surface and stained with Oil Red O, as previously described (25). The percent of aorta covered with

lesions was found to be significantly less in the mice injected with Ac-hE18A-NH_2 (42.18±4.29%) compared with the saline group (58.78±4.30%; p=0.013; Fig. 6b).

4. Discussion

Previous reports have shown that a single administration of Ac-hE18A-NH_2 derived by covalently attaching 141-150 region of apoE to a class A amphipathic helical peptide 18A significantly reduces plasma cholesterol levels in different dyslipidemic mouse and rabbit models (11–14). The mechanism was thought to be due to the peptide associating to the atherogenic apoB-containing lipoproteins, targeting them to the liver for excretion. However, the chronic effect of this peptide on plasma cholesterol levels has not been previously studied. To evaluate effects of multiple administrations of this peptide on plasma cholesterol levels and effects on atherosclerotic lesion, we designed a control peptide Ac-nhE18A-NH_2 derived from 150-161 region of apoE (nh represents non-heparin binding domain) covalently linked to 18A. While Ac-hE18A-NH_2 possesses a cationic nature, Ac-nhE18A-NH_2 has an overall net negative change. Helical net analysis of the structures of these two peptides show that while the Ac-hE18A-NH_2 has a twist in the nonpolar face, Ac-nhE18A-NH_2 possesses a class A amphipathic helical motif (Fig. 1; 27).

Both peptides effectively form complexes with phospholipids to essentially the same degree (Fig. 2a) and are able to associate with apoB-containing atherogenic lipoproteins as demonstrated by the change in agarose electrophoretic mobility (Fig. 2b). Ac-hE18A-NH_2 incubated with human HDL reduced monocyte binding to endothelial cells in culture while Ac-nhE18A-NH_2 did not (Fig. 3b), suggesting peptide Ac-hE18A-NH_2 reduced inflammatory properties of HDL in this assay. In addition, LDL incubated with Ac-hE18A-NH_2 had reduced lipid hydroperoxides, while LDL incubated with Ac-nhE18A-NH_2 had substantially increased LOOH (Fig. 3c). Ac-hE18A-NH_2 and not Ac-nhE18A-NH_2 mediated uptake of LDL by HepG2 cells (Fig. 3a) and clearance of lipoprotein cholesterol from the plasma of dyslipidemic mice (Fig. 4a), perhaps due to the latter peptide being unable to bind to cell surface HSPG. The involvement of proteoglycans in peptide-mediated lipoprotein clearance was demonstrated by pretreatment of mice with heparinase, which totally abolished peptide-mediated clearance (Fig. 4b). However, treatment with heparinase following injection of Ac-hE18A-NH_2 had no effect on peptide-mediated cholesterol clearance (Fig. 4c), suggesting that cleared peptide-lipoprotein complexes are no longer dependent on HSPG in a rapid process taking place within 15 minutes. *In vitro* [^{35}S]HSPG experiments demonstrated that Ac-hE18A-NH_2 did not inhibit heparinase activity on HepG2 cells in culture (Supplemental Fig. 1). Steps subsequent to HSPG binding by Ac-hE18A-NH_2-lipoprotein complexes have not yet been elucidated, except to demonstrate that the LDL receptor is not required for peptide-mediated clearance (12).

Administration of peptide Ac-hE18A-NH_2 three times a week intravenously in apoE null mice reduced plasma cholesterol and triglyceride levels significantly compared to either the control or Ac-nhE18A-NH_2 groups (Figs.5a and b). In addition, several *in vitro* and *in vivo* experiments show that this peptide is also anti-inflammatory (14). In contrast to Ac-hE18A-NH_2, Ac-nhE18A-NH_2 actually exhibited pro-inflammatory effects *in vitro* and in apoE null mice. Aortic sinus lesion size was decreased in older apo E null mice administered Ac-hE18A-NH_2 compared to the control group, and was significantly increased in the group administered Ac-nhE18A-NH_2 (Fig. 6a). Peptide Ac-hE18A-NH_2 also significantly decreased aortic *en face* lesions (Fig. 6b), increased PON-1 activity (Fig. 5c), and decreased LDL lipid hydroperoxides (Fig. 3c), while Ac-nhE18A-NH_2 exhibited opposite and pro-atherogenic properties.

It is surprising that the class A amphipathic helical peptide Ac-nhE18A-NH_2 exhibited pro-inflammatory and pro-atherogenic properties. Previously we have reported in a series of peptide analogs that a variation in the non-polar face of a prototypic peptide 2F to produce 3F, 4F, 5F, 6F and 7F analogs exhibited varying effects on the LDL-induced monocyte chemotaxis (28). The peptide 4F, with aromatic amino acids (including four Phe residues) clustered at the center of the nonpolar face, was the most effective analog. However, peptide analogs $3F^3$ and $3F^{14}$, in which Leu residues at the 3 or 14 positions in the linear sequence of the peptide 18A were replaced by Phe residues, were either ineffective or perhaps enhanced LDL-induced monocyte chemotaxis (28). In addition, comparison of the peptides 3F-2 (which possesses the same amino acids as peptide $3F^{14}$ but aromatic residues are clustered at the center of the nonpolar face) was able to inhibit LDL-induced monocyte chemotaxis and reduced lesion formation in apoE null mice, while peptide $3F^{14}$ was not effective (19,29). Physical chemical studies of these two peptides revealed that the inactive peptide $3F^{14}$ was more deeply buried in the lipid membrane, while the active peptide 3F-2 associated with the charged phospholipid headgroup (19). Based on these studies we propose that the makeup of the amino-terminal regions of these peptides differ in the charge and the twist of the helices, which may account for their different biological properties. The amino terminal cationic charges and disruption of the helix may cause Ac-hE18A-NH_2 to interact with the headgroup and penetrate the membrane less deeply, similarly to 3F-2, while Ac-nhE18A-NH_2, with a net charge of −1 and a more defined helix may penetrate more deeply, analogous to $3F^{14}$. This may give Ac-hE18A-NH_2 the ability to interact with and shield from oxidation the Sn-2 acyl chain of palmitoylarachidonoyl phosphatidylcholine (PAPC) or palmitoyllineoyl phosphatidylcholine (PLPC). In support of this, we show that while incubation of Ac-hE18A-NH_2 reduced lipid hydroperoxides on LDL, Ac-nhE18A-NH_2 actually increased LOOH levels (Fig. 3c).

In summary, we have shown that while addition of the 141-150 region of human apoE to the class A amphipathic helical peptide 18A produces Ac-hE18A-NH_2 which lowers plasma cholesterol levels and reduces lesion formation in apoE null mice, addition of the 151-160 region of human apoE to 18A produces a lipid-associating peptide that is pro-atherogenic, despite the presence of a class A amphipathic helical structure. Thus, lipid binding properties alone are not sufficient for atheroprotective properties of the class A amphipathic helical motif; some other factors such as are present in Ac-hE18A-NH_2 or as previously described (30,31), are essential for designing atheroprotective apolipoprotein mimetic peptides.

Supplementary Material

Refer to Web version on PubMed Central for supplementary material.

Acknowledgments

This study was supported by NIH grants P01 HL34343, R01 GM082952, and R01 HL0908030.

References

1. Piedrahita JA, Zhang SH, Hagaman JR, Oliver PM, Maeda N. Generation of mice carrying a mutant apolipoprotein E gene inactivated by gene targeting in embryonic stem cells. Proc Natl Acad Sci USA 1992;89:4471–4475. [PubMed: 1584779]
2. Nakashima Y, Plump AS, Raines EW, Breslow JL, Ross R. ApoE-deficient mice develop lesions of all phases of atherosclerosis throughout the arterial tree. Arterioscler Thromb Vasc Biol 1994;14:133–140.
3. Shimano H, Yamada N, Katsuki M, Yamamoto K, Gotoda T, Harada K, Shimada M, Yazaki Y. Plasma lipoprotein metabolism in transgenic mice overexpressing apolipoprotein E. Accelerated

clearance of lipoproteins containing apolipoprotein B. J Clin Invest 1992;90:2084–2091. [PubMed: 1430232]

4. Mahley RW, Weisgraber KH, Hussein MM, Greenman B, Fisher M, Vogel T, Gorecki M. Intravenous infusion of apolipoprotein E accelerates clearance of plasma lipoproteins in rabbits. J Clin Invest 1989;83:2125–2130. [PubMed: 2723074]
5. Grundy SM. Low-density lipoprotein, non-high-density lipoprotein, and apolipoprotein B as targets of lipid-lowering therapy. Circulation 2002;106:2526–2529. [PubMed: 12427645]
6. Mahley RW. Apolipoprotein E: cholesterol transport protein with expanding role in cell biology. Science 1988;240:622–630. [PubMed: 3283935]
7. Weisgraber KH. Apolipoprotein E: Structure-function relationships. Adv Protein Chem 1994;45:249–302. [PubMed: 8154371]
8. Bradley WA, Gilliam EB, Gotto AM Jr, Gianturco SH. Apolipoprotein E degradation in human very low density lipoproteins by protease(s): Chemical and biological consequences. Biochem Biophys Res Commun 1982;109:1360–1367. [PubMed: 6301435]
9. Datta G, Chaddha M, Garber DW, Chung BY, Tytler EM, Bradley WA, Gianturco SH, Anantharamaiah GM. The receptor binding domain of apolipoprotein E, linked to a model class A amphipathic helix, enhances internalization and degradation of LDL by fibroblasts. Biochemistry 2000;39:213–220. [PubMed: 10625496]
10. Anantharamaiah GM, Jones JL, Brouillette CG, Schmidt CF, Chung BH, Hughes TA, Bhown AS, Segrest JP. Studies of synthetic peptide analogs of the amphipathic helix. Structure of complexes with dimyristoyl phosphatidylcholine. J Biol Chem 1985;260:10248–10255. [PubMed: 4019510]
11. Datta G, Garber DW, Chung BH, Chaddha M, Dashti N, Bradley WA, Gianturco SH, Anantharamaiah GM. Cationic domain 141–150 of apoE covalently linked to a class A amphipathic helix enhances atherogenic lipoprotein metabolism in vitro and in vivo. J Lipid Res 2001;42:959–966. [PubMed: 11369804]
12. Garber DW, Handattu S, Aslan I, Datta G, Chaddha M, Anantharamaiah GM. Effect of an arginine-rich amphipathic helical peptide on plasma cholesterol in dyslipidemic mice. Atherosclerosis 2003;168:229–237. [PubMed: 12801605]
13. Gupta H, White CR, Handattu S, Garber DW, Datta G, Chaddha M, Dai L, Gianturco SH, Bradley WA, Anantharamaiah GM. Apolipoprotein E mimetic peptide dramatically lowers plasma cholesterol and restores endothelial function in Watanabe Heritable Hyperlipidemic rabbits. Circulation 2005;111:3112–3118. [PubMed: 15939819]
14. Datta G, White CR, Dashti N, Chaddha M, Palgunachari MN, Gupta H, Handattu SP, Garber DW, Anantharamaiah GM. Anti-inflammatory and recycling properties of an apolipoprotein mimetic peptide, Ac-hE18A-NH_2. Atherosclerosis 2010;208:131–141.
15. Cardin AD, Hirose N, Blankenship DT, Jackson RL, Harmony JAK, Sparrow DA, Sparrow JT. Binding of a high reactive heparin to human apolipoprotein E: Identification of two heparin-binding domains. Biochem Biophys Res Comm 1986;134:783–789. [PubMed: 3947350]
16. Palgunachari MN, Mishra VK, Lund-Katz S, Phillips MC, Adeyeye SO, Alluri S, Anantharamaiah GM, Segrest JP. Only the two end helixes of eight tandem amphipathic helical domains of human apo A-I have significant lipid affinity: Implications for HDL assembly. Arterioscler Thromb Vasc Biol 1996;16:328–338. [PubMed: 8620350]
17. Morrisett JD, David JSK, Pownall HJ, Gotto AM Jr. Interaction of an apolipoprotein (apoLP-alanine) with phosphatidylcholine. Biochemistry 1973;12:1290–1299. [PubMed: 4348832]
18. Schumaker VN, Puppione DL. Sequential flotation ultracentrifugation. Methods Enzymol 1986;128:155–170. [PubMed: 3724500]
19. Handattu SP, Garber DW, Horn DC, Hughes DW, Berno B, Bain AD, Mishra VK, Palgunachari MN, Datta G, Anantharamaiah GM, Epand RM. ApoA-I mimetic peptides with differing ability to inhibit atherosclerosis also exhibit differences in their interactions with membrane bilayers. J Biol Chem 2007;282:1980–1988. [PubMed: 17114186]
20. Goldstein JL, Basu SK, Brown MS. Receptor-mediated endocytosis of low-density lipoprotein in cultured cells. Methods Enzymol 1983;98:241–260. [PubMed: 6321901]
21. Lowry OH, Rosebrough NJ, Farr AL, Randall RJ. Protein measurement with the Folin phenol reagent. J Biol Chem 1951;193:265–275. [PubMed: 14907713]

22. El-Saadani M, Esterbauer H, El-Sayed M, Goher M, Nassar AY, Jurgens G. A spectrophotometric assay for lipid peroxides in serum lipoproteins using a commercially available reagent. J Lipid Res 1989;30:627–630. [PubMed: 2754343]

23. Ji ZS, Sanan DA, Mahley RW. Intravenous heparinase inhibits remnant lipoprotein clearance from the plasma and uptake by the liver: in vivo role of heparan sulfate proteoglycans. J Lipid Res 1995;36:583–592. [PubMed: 7539827]

24. Garber DW, Datta G, Chaddha M, Palgunachari MN, Hama SY, Navab M, Fogelman AM, Segrest JP, Anantharamaiah GM. A new synthetic class A amphipathic peptide analogue protects mice from diet-induced atherosclerosis. J Lipid Res 2001;42:545–552. [PubMed: 11290826]

25. Palinski W, Ord VA, Plump AS, Breslow JL, Steinberg D, Witztum JL. ApoE-deficient mice are a model of lipoprotein oxidation in atherogenesis. Demonstration of oxidation-specific epitopes in lesions and high titers of autoantibodies to malondialdehyde-lysine in serum. Arterioscler Thromb Vasc Biol 1994;14:605–616.

26. Anantharamaiah GM. Synthetic peptide analogs of apolipoproteins. Methods Enzymol 1986;128:627–647. [PubMed: 3724527]

27. Segrest JP, Garber DW, Brouillette CG, Harvey S, Anantharamaiah GM. The amphipathic α helix: A multifunctional structural motif in plasma apolipoproteins. Adv Protein Chem 1994;45:303–363. [PubMed: 8154372]

28. Datta G, Chaddha M, Hama S, Navab M, Fogelman AM, Garber DW, Mishra VK, Epand RM, Epand RF, Lund-Katz S, Phillips MC, Segrest JP, Anantharamaiah GM. Effects of increasing hydrophobicity on the physical-chemical and biological properties of a class A amphipathic helical peptide. J Lipid Res 2001;42:1096–1104. [PubMed: 11441137]

29. Datta G, Epand RF, Epand RM, Chaddha M, Kirksey MA, Garber DW, Lund-Katz S, Phillips MC, Hama S, Navab M, Fogelman AM, Palgunachari MN, Segrest JP, Anantharamaiah GM. Aromatic residue position on the nonpolar face of class A amphipathic helical peptides determines biological activity. J Biol Chem 2004;279:26509–26517. [PubMed: 15075321]

30. Anantharamaiah GM, Navab M, Reddy ST, Garber DW, Datta G, Gupta H, White CR, Handattu SP, Palgunachari MN, Chaddha M, Mishra VK, Segrest JP, Fogelman AM. Synthetic peptides: managing lipid disorders. Curr Opin Lipidol 2006;17:233–237. [PubMed: 16680027]

31. Anantharamaiah GM, Mishra VK, Garber DW, Datta G, Handattu SP, Palgunachari MN, Chaddha M, Navab M, Reddy ST, Segrest JP, Fogelman AM. Structural requirements for antioxidative and anti-inflammatory properties of apolipoprotein A-I mimetic peptides. J Lipid Res 2007;48:1915–1923. [PubMed: 17570869]

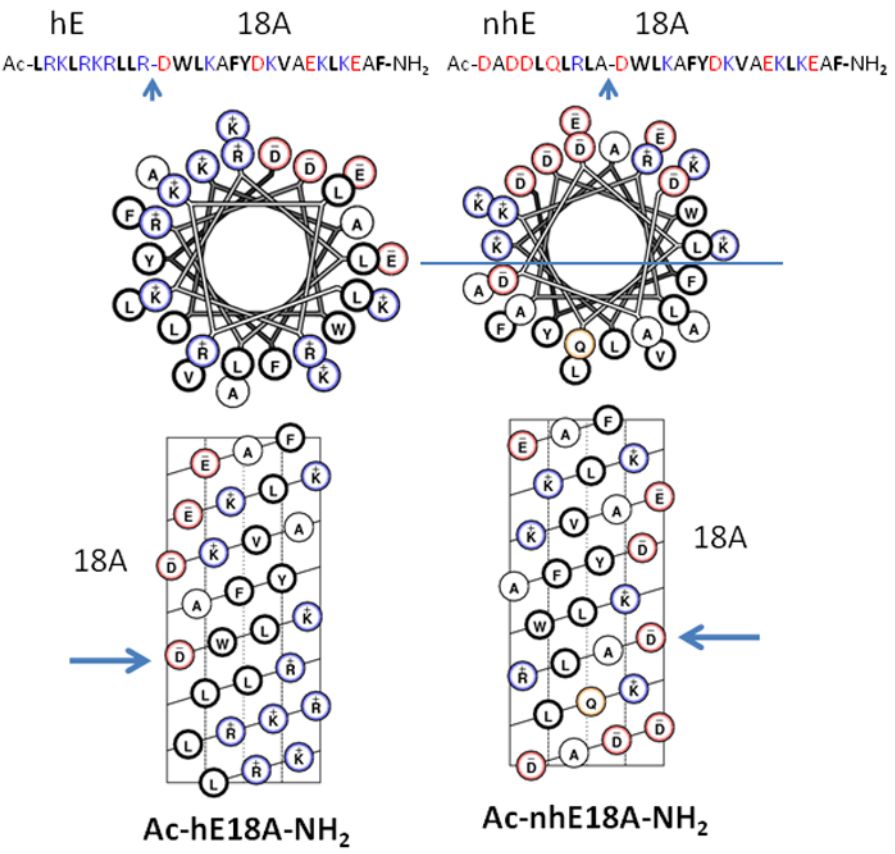

Fig. 1. Helical wheel and helical net representation of Ac-hE18A-NH_2 and Ac-nhE18A-NH_2

Blue arrow marks represent the point of attachment of hE (LRKLRKRLL, 141-150 region of human apoE) or (DADDLQLRLA, 151 to 160 region of human apoE) sequence to 18A (DWLKAFYDKVAEKLKEAF) a class A amphipathic helical peptide sequence (9). Helical net representation of Ac-hE18A-NH_2 shows a twisted nonpolar face at the bottom end (N-terminus) of the helical net, resulting in an apparent loss of amphipathic structure whereas, in both helical wheel and helical net representations, Ac-nhE18A-NH_2, shows a class A amphipathic helical structure (a well-separated polar-nonpolar face represented by a demarcation line in the helical wheel representation of Ac-nhE18A-NH_2) with a wide nonpolar face rich in Leu residues.

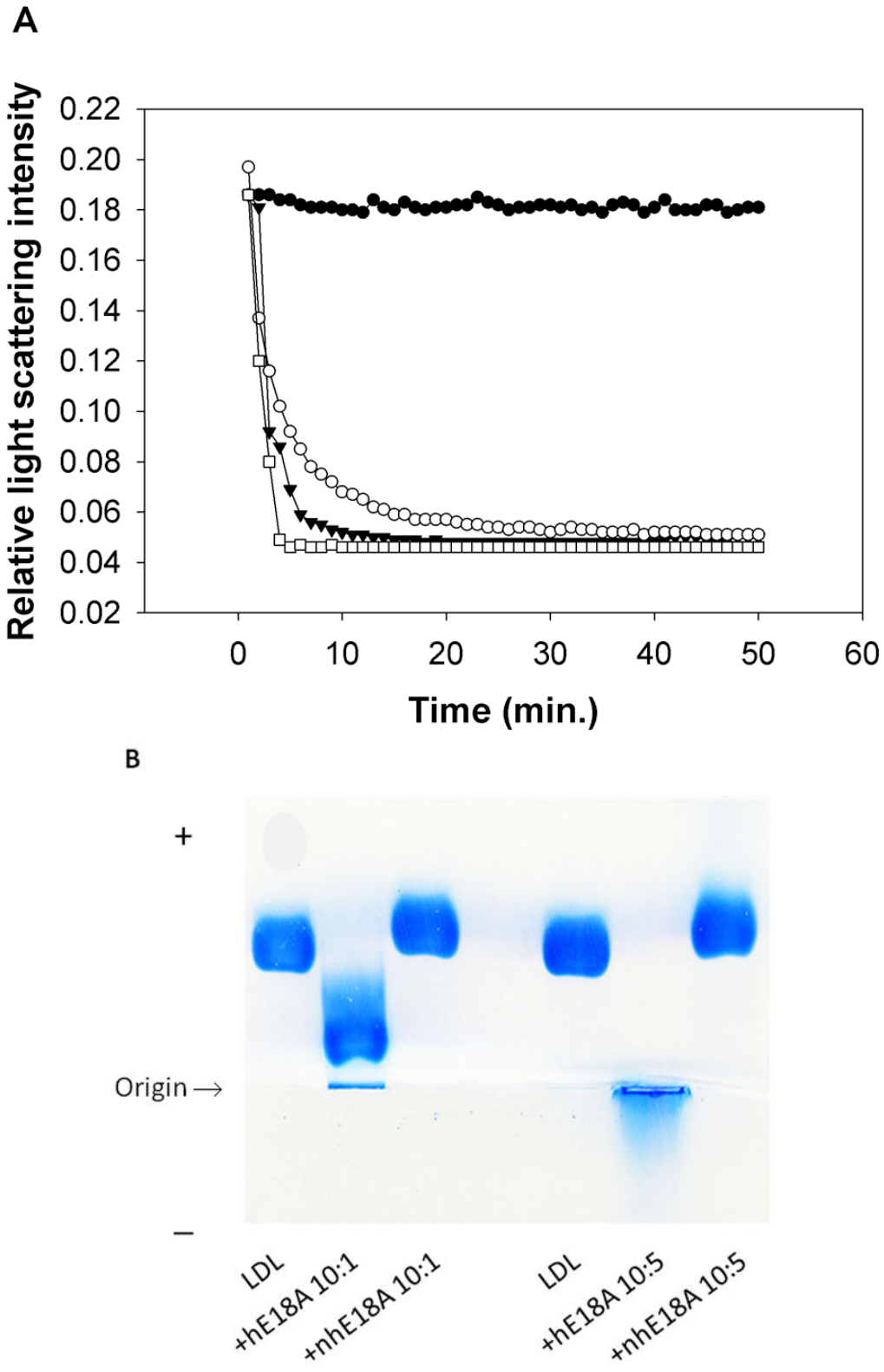

Fig. 2. Association of peptides with lipids and lipoproteins

a) Both Ac-hE18A-NH_2 and Ac-nhE18A-NH_2 clarify POPC suspensions. A representative POPC clarification curve of the relative right angle light scattering of the dissolution of POPC MLVs by peptides as a function of time is shown. An equimolar concentration of peptide and POPC (100 μM) was monitored at 400 nm. POPC (●), Ac-nhE18A-NH_2 (○), Ac-hE18A-NH_2 (▼), and Triton X-100 (□). **b)** Agarose gel electrophoresis of LDL ± Ac-hE18A-NH_2 and Ac-nhE18A-NH_2. LDL (10 μg; Lanes 1 and 4) was incubated with each peptide at a ratio of either 10:1 LDL:peptide w:w (lanes 2 and 3 or 10:5 (lanes 5 and 6) at 37°C for 30 min, electrophoresed on a 0.75% agarose gel, and stained with Coomassie Blue. In this and all subsequent figures, peptide abbreviations are as follows: hE18A: Ac-hE18A-NH_2; nhE18A; Ac-nhE18A-NH_2.

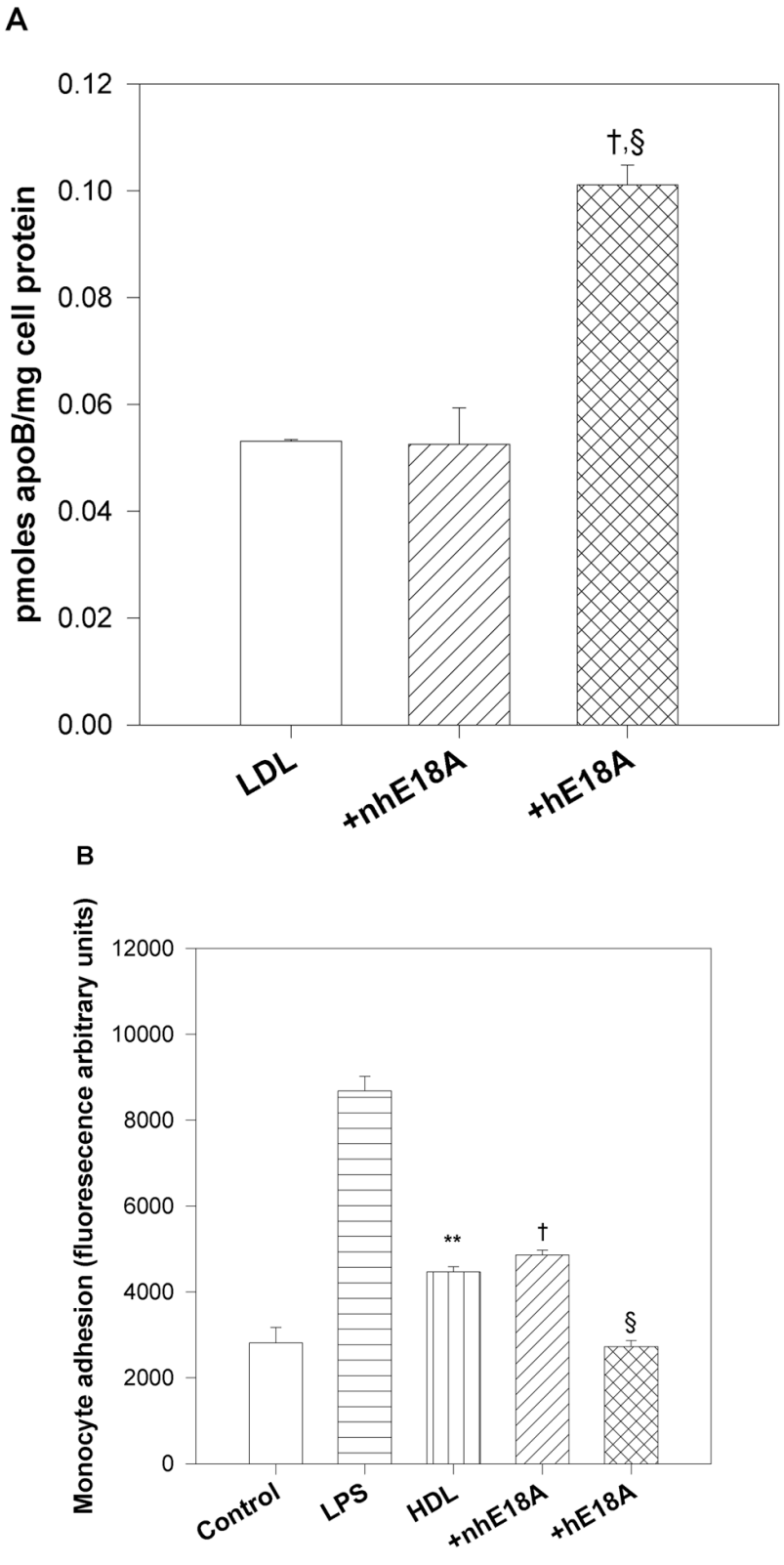

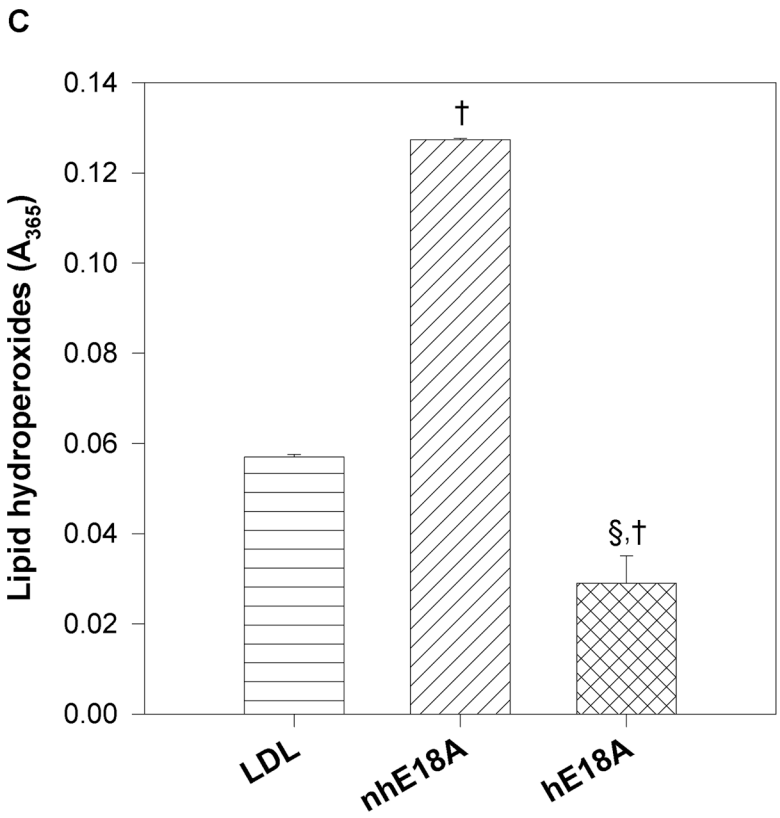

Fig. 3.

a) Peptide Ac-hE18A-NH_2 and not Ac-nhE18A-NH_2 mediates LDL uptake by HepG2 cells: Human [^{125}I] LDL was treated with either Ac-nhE18A-NH_2 or Ac-hE18A-NH_2. Cells that were treated with vehicle served as control. Ac-hE18A-NH_2 treated cells increased uptake of ^{125}I-LDL by approximately 100% compared to control cells, whereas uptake was similar to control cells when treated with Ac-nhE18A-NH_2. $^{\dagger}p<0.001$ vs controls; $^{\S}p<0.001$ vs Ac-nhE18A-NH_2; replicate measurements of three independent experiments. **b) Ac-hE18A-NH_2 inhibits monocyte adhesion to bovine aortic endothelial cells (BAEC):** BAECs were incubated with no additions (control), lipopolysaccharide (LPS) as a positive control, untreated human HDL, or with HDL isolated from human blood treated with either Ac-nhE18A-NH_2 or Ac-hE18A-NH_2. Calcein fluorescence of bound monocytes was read on a plate reader. Pre-treatment of HDL with Ac-hE18A-NH_2 inhibited monocyte adhesion to BAECs significantly, compared to either LPS treatment or HDL treated with Ac-nhE18A-NH_2. $^{**}p<0.01$ vs control; $^{\dagger}p<0.001$ vs control; $^{\S}p<0.001$ vs Ac-nhE18A-NH_2. **c) Effect of peptides on LDL lipid hydroperoxides.** Human LDL was isolated by ultracentrifugation and incubated with saline, Ac-nhE18A-NH_2, or Ac-hE18A-NH_2 overnight at 37° at a ratio of 10:1 LDL:peptide w/w. Lipid hydroperoxides were measured in triplicate by the CHOD-iodide method and the results are expressed as mean ± SEM. $^{\dagger}p<0.001$ vs control; $^{\S}p<0.001$ vs Ac-nhE18A-NH_2. Abbreviations are as described in Figure 2.

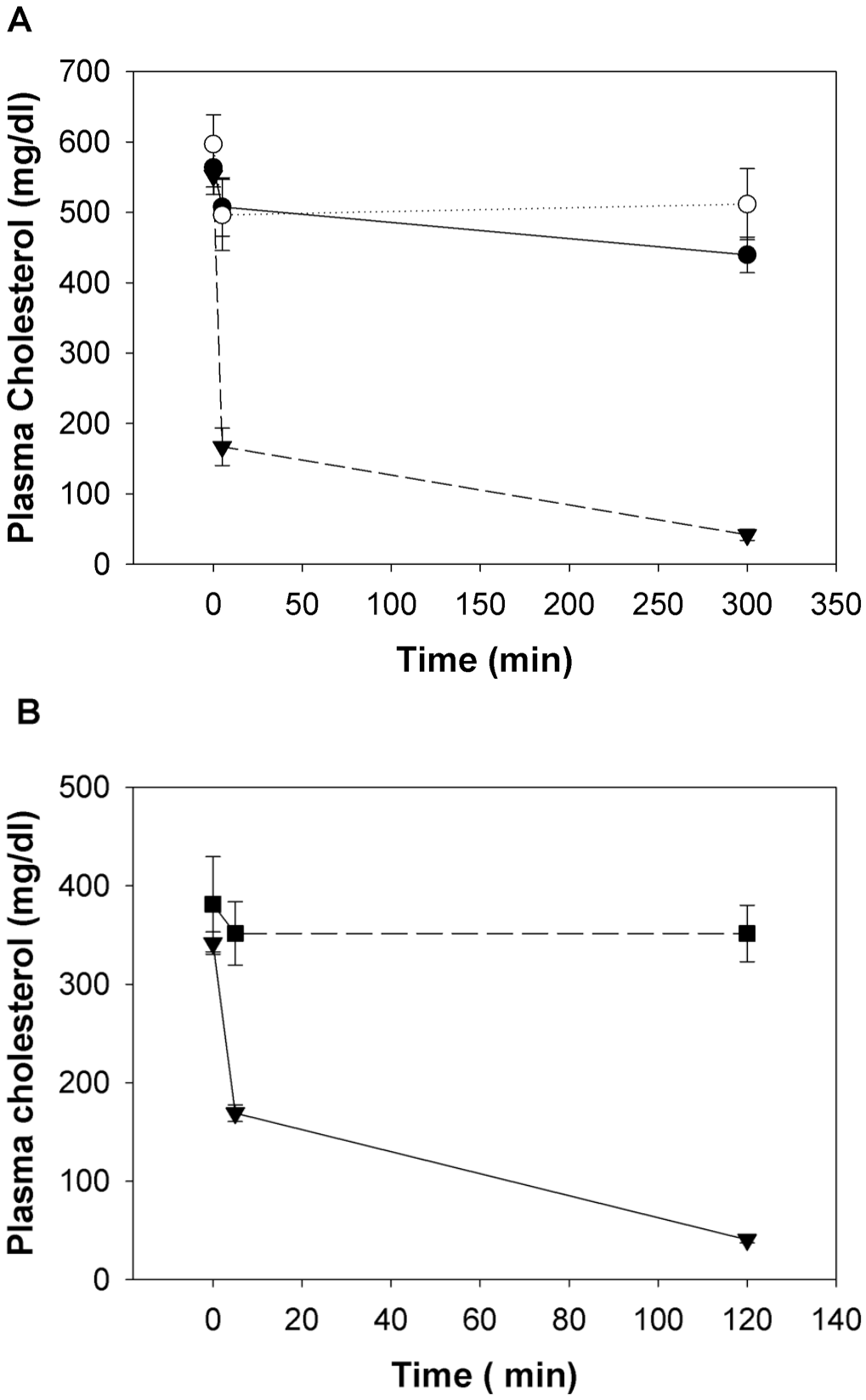

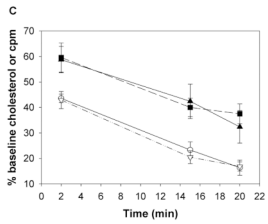

Fig 4. Acute administration of Ac-hE18A-NH_2 lowers plasma cholesterol levels and is HSPG mediated

a) Apo E null mice were administered either Ac-nhE18A-NH_2 (○) or Ac-hE18A-NH_2 (▼) (both peptides at 100 μg/mouse in 100 μL, retro-orbitally). Saline administered mice (●) served as controls. Ac-hE18A-NH_2-administered mice showed a significant decrease in plasma cholesterol levels both at 5 min and 5 hrs. post administration compared to the other two groups. Plasma cholesterol levels of Ac-nhE18A-NH_2 administered mice were not different from saline administered mice at any time point. N=5 in each group. **b)** The involvement of proteoglycans in Ac-hE18A-NH_2-mediated clearance of plasma cholesterol was tested by pre-injection of heparinase (i.v.; 50 U/mouse, ■) or saline (▼) five minutes before injection of peptide (i.v.; 100 μg/mouse) into apo E null mice (n=5). Pre-injection with heparinase essentially abolished the peptide-mediated clearance of plasma cholesterol. **c)** Post-injection of heparinase has no effect on cholesterol lowering ability of Ac-hE18A-NH_2. ApoE null mice were administered with [^{125}I]Ac-hE18A-NH_2 (100μg/mouse, iv) followed 15 min later either by saline (solid lines) or heparinase (dashed lines; 50 U/mouse). Plasma cholesterol levels (■, ▼) were decreased to a similar extent in both groups. Also, both groups showed identical disappearance of labeled peptide from plasma (○, ▽). N=6 in each group. Values are expressed as Mean ± SEM. Abbreviations are as described in Figure 2.

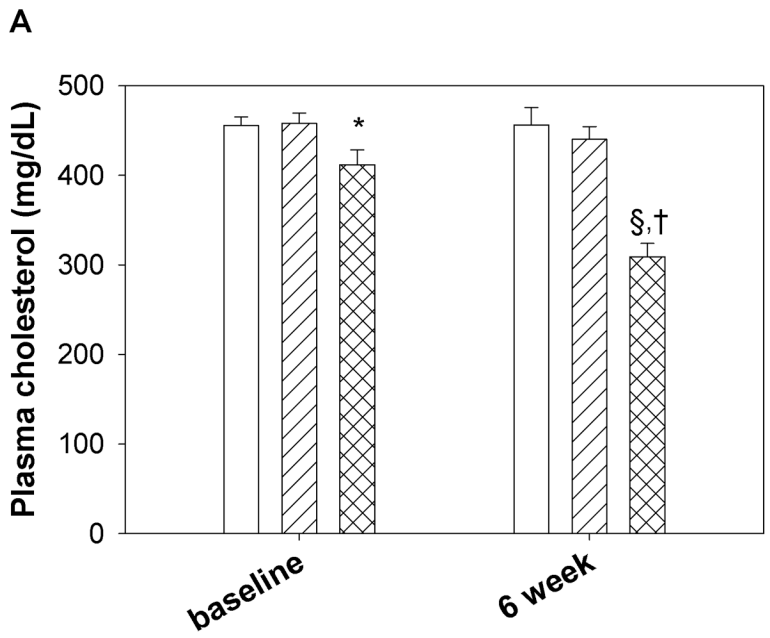

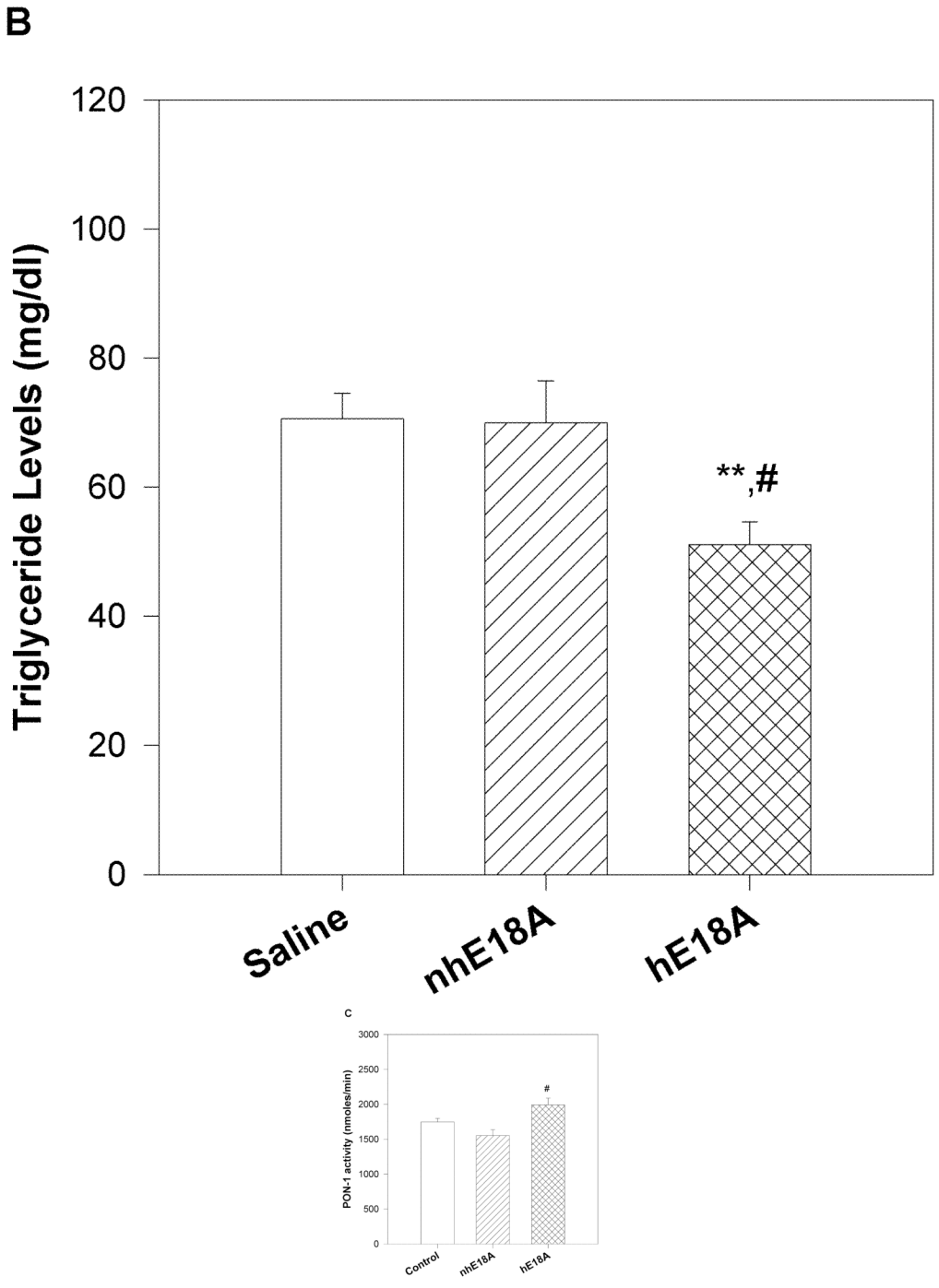

Fig. 5. Chronic administration of the peptide Ac-hE18A-NH_2 decreases plasma cholesterol and triglyceride, and improves PON-1 activity

16 week old female apo E null mice were administered with saline (open bar, n=14), Ac-nhE18A-NH_2 (cross hatch, n= 14), or Ac-hE18A-NH_2 (double hatch, n=12) retro-orbitally. 100 μg of each peptide in 100ul saline was administered 3 times a week for 6 weeks. At the end of six weeks and one day after the final injections, plasma was analyzed for cholesterol and triglyceride levels and PON-1 activity. **a)** After 6 weeks of treatment plasma from mice treated with Ac-hE18A-NH_2 showed significantly lower cholesterol levels compared to the

control group ($^{\dagger}p<0.001$ vs baseline and final controls and baseline Ac-hE18A-NH_2 levels, and $^{\S}p<0.001$ vs Ac-nhE18A-NH_2 final levels.), whereas there was no difference in plasma cholesterol levels of either saline or Ac-nhE18A-NH_2 treated mice. **b)** At the end of six weeks of peptide treatment, triglyceride levels were significantly reduced in the Ac-hE18A-NH_2 group compared with either controls (**$p<0.01$) or the Ac-hE18A-NH_2 group (#$p<0.01$). **c)** At the end of six-weeks, plasma from mice treated with Ac-hE18A-NH_2 had significantly higher PON-1 activity compared with Ac-nhE18A-NH_2 ($^{\#}p<0.01$ vs Ac-nhE18A-NH_2). Abbreviations are as described in Figure 2.

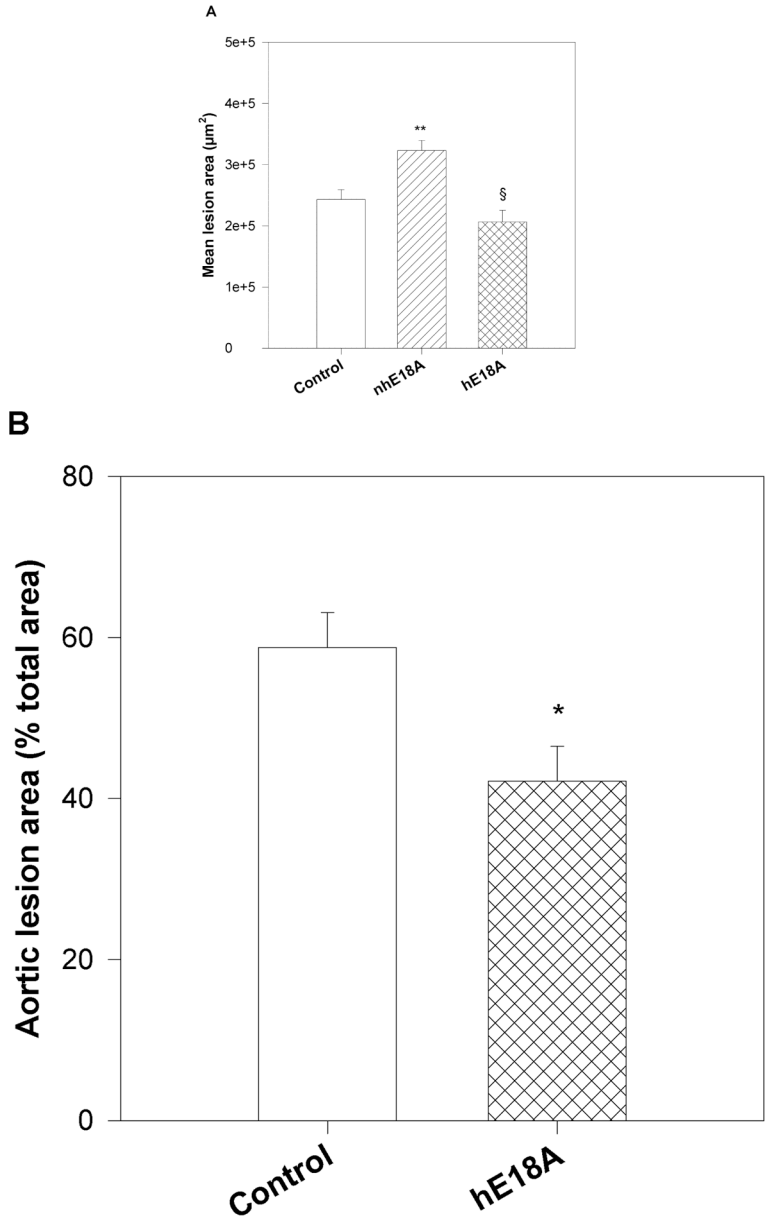

Fig. 6. Peptides Ac-nhE18A-NH_2 and Ac-hE18A-NH_2 have opposite effects on atherosclerotic lesion inhibition

a) Quantification of aortic sinus lesions. Treatment groups described in Fig. 4 were assessed for aortic sinus atherosclerotic lesions. Oil Red O stained areas in the aortic sinus were measured in all three groups at the end of treatment period. After 6 weeks of treatment, mice treated with peptide Ac-hE18A-NH_2 (double hatched bar) had significantly less atherosclerotic lesion areas compared with Ac-nhE18A-NH_2-administered mice (single hatched bar; $^{\S}p<0.001$ vs Ac-nhE18A-NH_2) while Ac-nhE18A-NH_2-administered mice had significantly greater lesion areas than controls (open bars; $^{**}p<0.01$ vs control). Data are expressed as mean ±S.E.M. **b) Quantification of *en face* lesions.** In a separate experiment, 22 week old female apo E null mice were administered saline (open bars; n=11) or Ac-hE18A-NH_2 (double hatched bars; n=12) for four weeks, three times per week. Mice were administered physiological saline solution or saline containing Ac-hE18A-NH_2 (100μg/100 μl) during the treatment period. Aortas were removed and pinned open from the aortic arch

to the iliac bifurcation and stained with Oil Red O. Total aortic area and area of Oil Red O staining were measured, and *en face* lesions were expressed as percent of total aortic area. Results are expressed as mean ± SEM. *$p<0.05$ vs control. Abbreviations are as described in Figure 2.

Table 1

Physical characteristics of Ac-hE18A-NH_2 and Ac-nhE18A-NH_2

	Ac-hE18A-NH_2	**Ac-nhE18A-NH_2**
Molecular Wt. (Da)	3576	3368
Hydrophobic moment/Residue	1.29	2.72
Corrected hydrophobicity of the nonpolar face	13.8	8.3
Overall hydrophobicity/Residue	−3.84	−3.54
Predicted lipid affinity (λ4)	9.57	10.30
Net charge	+6	−1